Kingdom of Saudi Arabia

Al-Imam Muhammad Ibn Saud Islamic University

College of Sciences

Department of Physics

Calculation of photon interaction probabilities in shielding glass materials

A graduation project submitted to the Department of Physics in partial fulfillment of the requirements for the degree of Bachelor of Science in Applied Physics

by

Ali Turki Alghamdi

Supervisor

Pro. Dr. Ahmed M. El-Khayatt

AIMISIU/COS/DOP/

Riyadh- KSA- 1446 H. - 2025 G.

Table of Contents

List of Tables

List of Figures

الإهداء

إلى من كانت دعواتهم سرّ نجاحي، وسندهم طريقي للتميز، والديَّ الحبيبين، نبض قلبي، ونور حياتي، لكم كل الحب والامتنان.

إلى أساتذتي الكرام، الذين كانوا شعلة تضيء دربي، وزرعوا فيّ حب العلم والمعرفة، شكرًا لعطائكم اللامحدود.

إلى إخوتي وأصدقائي، من شاركوني لحظات التعب والإنجاز، وكانوا لي خير رفاق الدرب، أُهديكم كل التقدير والمودة.

وأخيرًا، إلى كل من دعمني، ووقف بجانبي، وأمن بقدراتي، هذا العمل ثمرة جهدٍ أهديه إليكم بكل فخر واعتزاز.

الشكر

نشكر الله مولانا وخالقنا الذي من علينا بإتمام هذا العمل المتواضع مع رجائنا أن يتقبله منا ويجعله خالصاً لوجهه الكريم ، وإيمانا بفضل الاعتراف بالجميل وتقديم الشكر والامتنان لأصحاب المعروف فإننا نتقدم بالشكر الجزيل والثناء العظيم لكل من ساعد في إنجاح هذه المشروع وأخص بالذكر: أستاذنا ومشرفنا الفاضل الاستاذ الدكتور أحمد الخياط حفظه الله على الإشراف على هذا البحث ومتابعته له منذ الخطوات الأولى وعلى ما منحنا من صدر واسع ونصح وإرشاد ساعد على إخراج هذا العمل بهذه الصورة. نسأل الله أن يجزيه عنا خير الجزاء. كما نتقدم بالشكر الجزيل لوالدينا العزيزين حفظهم الله على تشجيعهم ومساعدتهم لنا حتى أتممنا بحثنا هذا. وختاما نأمل من الله أن نكون قد وفقنا في إعداد هذا البحث بالطريقة التي تنفع المجتمع وأن ننال رضى الله عز وجل.

ملخص

تم في هذه الدراسة تحليلًا مفصلًا لاحتمالات التوهين النسبي المرتبطة بتفاعلات الفوتونات الجزئية التي تحدث داخل نظام زجاجي مكون من خمسه تركيبات. تهدف هذه الدراسة على وجه التحديد إلى تحديد نقاط تساوي الاحتمالية - المشار إليها بنقاط التوازن - بين أنواع مختلف التفاعلات الجزئية، وهي تأثير الفوتوضوئي وتشتت كومبتون، بالإضافة الي تفاعل إنتاج الازواج. لتحقيق هذا الهدف، تم حساب معاملات التوهين الخطي،،وسمك نصف القيمة عبر مدي طويل من طاقات الفوتونات. علاوة على ذلك، فحصت الدراسة تاثير آاستبدال P_2O_5 بـ Fe_2O_3داخل نظام الزجاج المحدد ($(35-x)\ P_2O_5\text{-}x\ Fe_2O_320\ (CaO\text{-}20CoCl_2\text{-}25B_2O_3$)، حيث تأخذ x قيم 0، 4، 8، 11، و15 بالمئة وزناً. وأدي هذا الاستبدال إلى تغيير تكوين الزجاج، كما عزز أيضًا من قدرة امتصاص الفوتونات لدى الزجاج. تشير نتائج هذه الدراسة إلى أن استبدال P_2O_5 بـ Fe_2O_3 يعزز بشكل كبير من قدرة التوهين لأشعة الجاما لنظام الزجاج تحت الدراسة. نتيجة لهذا التعزيز، تلاحظ الدراسة زيادة في قيم معامل التوهين الخطي(μ) ، و انخفاض في قيم طبقة نصف القيمة(HVL) المقابلة، وكما حدث انحراف ملحوظ في نقاط التوازن المحددة للاحتمالات الجزئية لتفاعل الفوتونات ضمن سياق نظام الزجاج المعني. تؤكد هذه النتائج أهمية تكوين المادة في تأثير ديناميات تفاعل الفوتونات.

Abstract

This study conducts a detailed analysis of the relative attenuation probabilities associated with partial photon interactions that occur within a five-glass system. The research specifically aims to identify points of equal probability—referred to as balance points— between different types of interactions, namely the photoelectric effect and Compton scattering, as well as between Compton interactions and pair production. To achieve these objectives, the study calculates linear attenuation coefficients, which provide insights into the material's effectiveness at reducing radiation transmission, and half-value layers across a diverse range of photon energies. Furthermore, the investigation thoroughly examines the implications of substituting P_2O_5 with Fe_2O_3 within the specific glass system designated as 20CaO-20$CoCl_2$-25B_2O_3 (35-x) P_2O_5-x Fe_2O_3, where x takes on values of 0, 4, 8, 11, and 15 weight percent. This substitution not only serves to alter the composition of the glass but also plays enhanced the glass photon attenuation capacity. The findings of this comprehensive analysis indicate that replacing P2O5 with Fe2O3 significantly enhances the attenuation capacity of the glass system. As a result of this modification, the study observes an increase in the values of the linear attenuation coefficient (μ), a corresponding decrease in half-value layer (HVL) values, and a notable shift in the established balance points of the partial interaction probabilities within the context of the glass system in question. These outcomes underscore the importance of material composition in influencing photon interaction dynamics

Notations

Symbol	Explanation	Unit
$h\upsilon$	Incident photon energy	eV
K.E	Kinetic energy	eV
B.E	Binding energy	eV
$h\upsilon'$	Reduced energy	eV
θ	Angle of photon scattered	Degree
φ	Angle of electron recoils	Degree
x_i	Represents the mole fraction	-
M_i	Molecular mass of the ith raw material.	-
μ	Linear attenuation coefficient of the material	cm^{-1}
μ_m	Mass attenuation coefficient of the material	cm^2/g
ρ	Density of the absorber	g/cm^3
I_0	Initial intensity of the beam before entering the material	-
I	Intensity after passing through a distance x in the material	-
x	Thickness of the material that the photons are traveling through	-
σ_C	Total Compton cross section for a single electron	cm^2/e
W_i	Represents the weight fraction	g
k_i	Number of atoms of the element	-
A	Molecular weight of the compound	-

ملخص

تجري هذه الدراسة تحليلًا مفصلًا لاحتمالات التوهين النسبي المرتبطة بتفاعلات الفوتونات الجزئية التي تحدث داخل نظام زجاجي مكون من خمسة تركيبات. تهدف هذه الدراسة على وجه التحديد إلى تحديد نقاط تساوي الاحتمالية - المشار إليها بنقاط التوازن - بين أنواع مختلف التفاعلات الجزئية، وهي تأثير الفوتوضوئي وتشتت كومبتون، بالإضافة الي تفاعل إنتاج الازواج. لتحقيق هذا الهدف، تم حساب معاملات التوهين الخطي، ، وسمك نصف القيمة عبر مدي طويل من طاقات الفوتونات. علاوة على ذلك، فحصت الدراسة تاثير آاستبدال P_2O_5 بـ Fe_2O_3 داخل نظام الزجاج المحدد ($20\ (35\text{-}x)\ CaO\text{-}20CoCl_2\text{-}25B_2O_3$ $(P_2O_5\text{-}x\ Fe_2O_3)$، حيث تأخذ x قيم 0، 4، 8، 11، و15 بالمئة وزناً. وأدي هذا الاستبدال إلى تغيير تكوين الزجاج ، كما عزز أيضًا من قدرة امتصاص الفوتونات لدى الزجاج. تشير نتائج هذه الدراسة إلى أن استبدال P_2O_5 بـ Fe_2O_3 يعزز بشكل كبير من قدرة التوهين لاشعة الجاما لنظام الزجاج تحت الدراسة. نتيجة لهذا التعزيز، تلاحظ الدراسة زيادة في قيم معامل التوهين الخطي(μ) ، و انخفاض في قيم طبقة نصف القيمة(HVL) المقابلة، وكما حدث انحراف ملحوظ في نقاط التوازن المحددة للاحتمالات الجزئية لتفاعل الفوتونات ضمن سياق نظام الزجاج المعني. تؤكد هذه النتائج أهمية تكوين المادة في تأثير ديناميات تفاعل الفوتونات.

Abstract

This study conducts a detailed analysis of the relative attenuation probabilities associated with partial photon interactions that occur within a five-glass system. The research specifically aims to identify points of equal probability—referred to as balance points—between different types of interactions, namely the photoelectric effect and Compton scattering, as well as between Compton interactions and pair production. To achieve these objectives, the study calculates linear attenuation coefficients, which provide insights into the material's effectiveness at reducing radiation transmission, and half-value layers across a diverse range of photon energies. Furthermore, the investigation thoroughly examines the implications of substituting P_2O_5 with Fe_2O_3 within the specific glass system designated as 20CaO-20$CoCl_2$-25B_2O_3 (35-x) P_2O_5-x Fe_2O_3, where *x* takes on values of 0, 4, 8, 11, and 15 weight percent. This substitution not only serves to alter the composition of the glass but also plays enhanced the glass photon attenuation capacity. The findings of this comprehensive analysis indicate that replacing P_2O_5 with Fe_2O_3 significantly enhances the attenuation capacity of the glass system. As a result of this modification, the study observes an increase in the values of the linear attenuation coefficient (μ), a corresponding decrease in half-value layer (HVL) values, and a notable shift in the established balance points of the partial interaction probabilities within the context of the glass system in question. These outcomes underscore the importance of material composition in influencing photon interaction dynamics.

Chapter 1: Introduction

Photon radiation, recognized for its penetrating properties, is widely employed across various fields, including industrial applications, radiation protection, dosimetry, and medical uses such as diagnostic imaging, therapeutic techniques, and sterilization protocols, among others. As a form of indirect ionizing radiation, photons engage with the electrons of atoms and molecules in materials, resulting in ionization and excitation processes. These interactions of gamma ray thoroughly documented and analyzed in scientific literature(El-Khayatt, 2017a, 2017b, 2017c, 2011; El-Khayatt and Saudy, 2020). The degree of photon irradiation is addressed through radiation interaction parameters, including mass attenuation coefficients and mass absorption coefficients. In the following section, we summarize the various interaction processes of gamma rays with matter.

1.1. Interactions of Photons with Matter

Photons are massless, electrically neutral electromagnetic radiation that travel at the constant speed of light, c. Because they carry no charge, they do not lose energy through Coulombic interactions with atomic electrons, unlike charged particles. As a result, photons can travel long distances before their energy is partially or fully transferred to electrons, which then deposit this energy in the medium. Energy loss occurs through mechanisms such as the photoelectric effect, Compton scattering, and pair production.

1.1.1. Photoelectric effect (low energies and high Z)

In the photoelectric absorption process, a photon interacts with an absorber atom, resulting in the complete disappearance of the photon. In its place, an energetic photoelectron is emitted from one of the atom's bound shells (inner shells: K, L, and M). The emitted electrons absorb all the energy from the incoming photon, hv. A portion of this energy is used to overcome the electron's binding energy, while the remaining energy contributes to the kinetic energy of the electron as it is released from the atom.

$$K.E = hv - b.e \tag{1.1}$$

The photoelectric process is the primary mechanism of photon interaction at relatively low photon energies and high atomic numbers (Z).

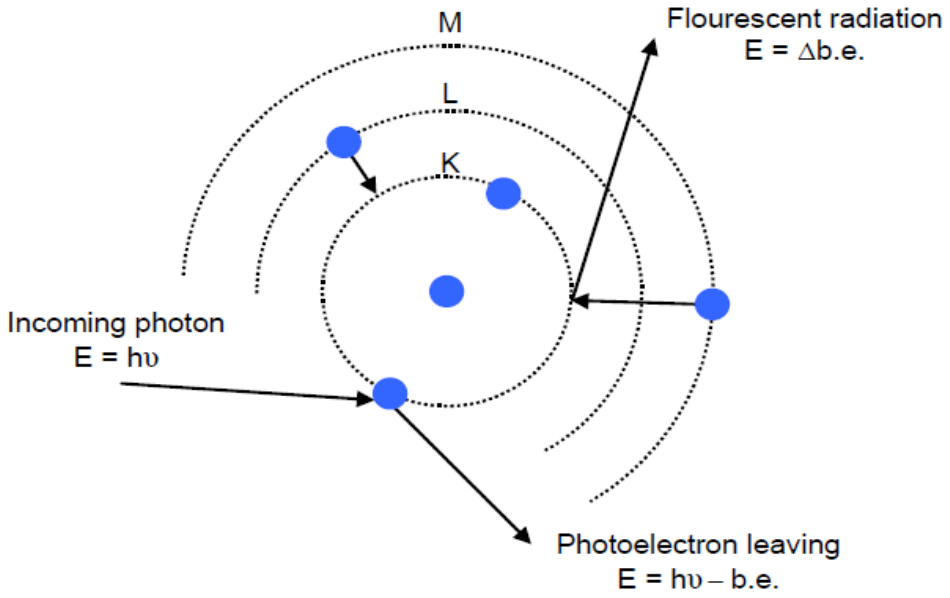

Figure 1.1: The photoelectric effect

1.1.2. Compton scatter (incoherent scattering) (in medium energies)

When high-energy photons fall, exceeding the threshold for the photoelectric effect, the emission of electrons occurs alongside the scattering of the remaining photons. Compton (1923) proposed that photons interact with matter by behaving as particles that collide with electrons.

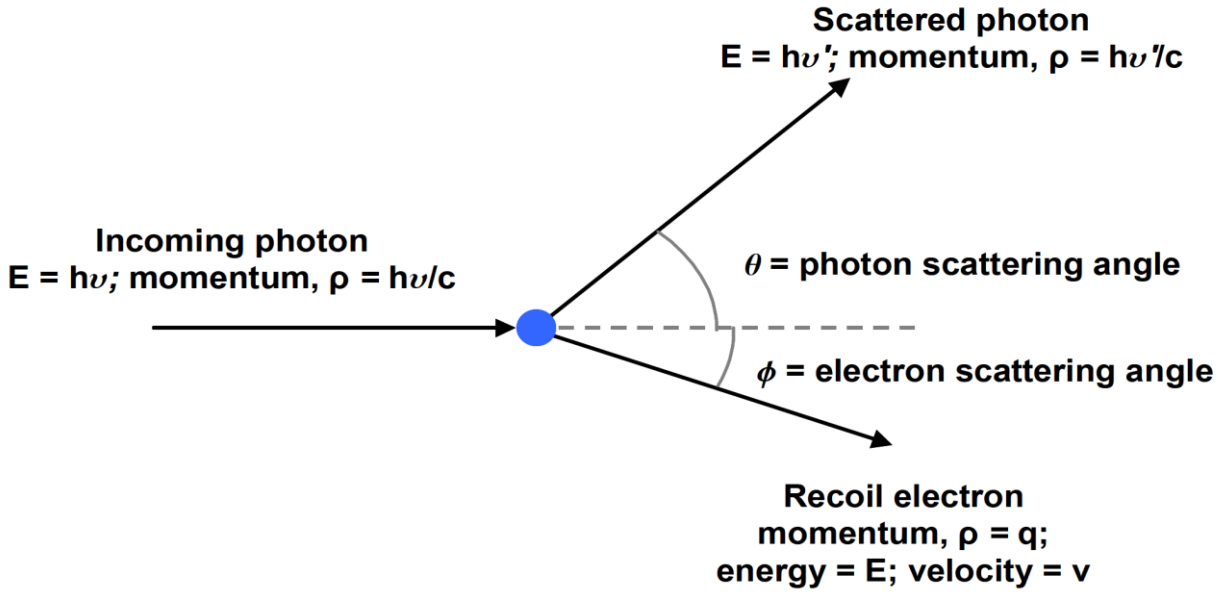

Figure 1.2: The Compton (incoherent scattering)

In the Compton process, a photon interacts with an atomic electron as if it were a "free" electron. Here, "free" indicates that the electron's binding energy is significantly

lower than the energy of the incoming photon. During this interaction, the electron absorbs energy from the photon and is emitted at an angle θ. The photon, after this encounter, has its energy reduced and is scattered at the same angle θ.

Key characteristics of these interactions include: (1) all scattering angles are permitted, (2) the energy transferred to the electron can range from zero to a substantial portion of the gamma-ray energy, and (3) this mechanism is the most prevalent interaction in tissues for photon energies between 100 keV and 10 MeV. The likelihood of Compton scattering is nearly independent of the atomic number Z and decreases as the energy of the photon increases.

This phenomenon was first observed by Arthur Holly Compton in 1923 at the University of Washington, leading to his receipt of the Nobel Prize in Physics in 1927. The significance of the Compton Effect lies in its demonstration that the behavior of light cannot be entirely explained as a wave phenomenon.

1.1.3. Pair Production (in high energies)

When a photon with energy greater than 1.022 MeV interacts with matter, it can undergo a process known as pair production. As the photon approaches the nucleus of an atom, it experiences significant field effects from the nucleus. This interaction can cause the photon to vanish and subsequently re-emerge as a pair of electrons: one negative (e^-) and one positive (e^+). The kinetic energy of this electron pair will be the difference between the energy of the incoming photon and the total energy equivalent of the two electron masses (2 × 0.511 MeV, which equals 1.022 MeV).

$$E_{e^+} + E_{e^-} = h\nu - 1.022 \text{ (MeV)} \quad (1.2)$$

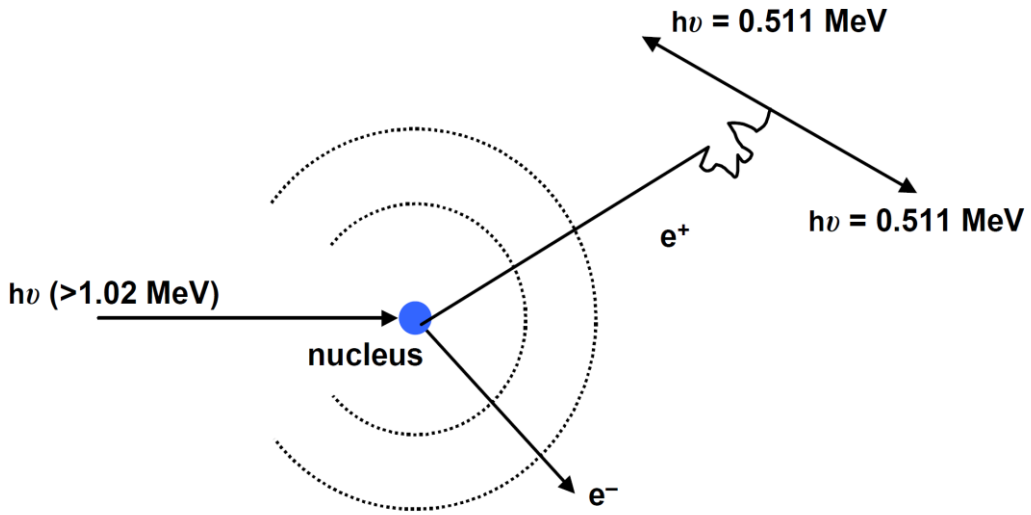

Figure 1.3: The pair production process.

Photon interactions with matter depend on their energy levels, with different processes becoming dominant at specific ranges. For instance, Compton scattering predominates around 1 MeV, the photoelectric effect is most significant at lower energies, and pair production is more likely at higher energies. The relative interaction probability quantifies how likely a photon is to undergo each of these interactions at a given energy. Calculating the relative probabilities of partial photon interactions in various materials is essential for understanding photon behavior in numerous scientific applications, such as medical imaging and radiation therapy. The likelihood of a photon undergoing coherent scattering, photoelectric absorption, incoherent (Compton) scattering, or pair production in a nuclear or electronic field within a material at a specific energy is defined by its relative interaction probability. These calculations typically involve the attenuation coefficients and cross-sections for different photon energies, utilizing programs like XCom (Gerward et al., 2001) and NXcom (El-Khayatt, 2011). For example, studies by El-Khayatt and Saudy (2018) have shown why the HVL values are nearly identical for all the examined samples at intermediate photon energies. They attributed this behavior to the relative dominance of Compton scattering and pair production in this energy region (El-Khayatt & Saudy, 2020).

1.2. Aim of the work

This study calculates the relative probabilities of partial photon interactions in five glass samples across a broad energy range of 10 keV to 100 MeV. These probabilities were derived from the NXcom computer program(El-Khayatt, 2011), based on data tabulated by Hubbell and Seltzer (1995) (Hubbell and Seltzer, 1995).

Chapter 2: Material and methods

2.1. Glass Preparation

In the present work a five-glass system 20CaO-20$CoCl_2$-25B_2O_3 (35-*x*) P_2O_5-*x* Fe_2O_3 (*x*=0,4, 8, 11, and 15 wt. %). $x = 0, 4, 8, 11, 15$ prepared by using melt quenching method. Following the melt quenching protocol, the amount of raw material (w_a) was calculated using the formula $w_a = x_a M_a / \sum_i x_i M_i$, where x_i represents the mole fraction and M_i is the molecular mass of the ith raw material. The mixtures were heated to 1200°C at a rate of 5°C/min, held at that temperature for 3 hours, and then cast into stainless-steel molds to form glass discs, which were later annealed in a furnace at 450°C for 2 hours. The samples were gradually cooled to room temperature. The chemical compositions and densities of the samples are presented in Tables 1 and 2, respectively.

Table 1.2: Density values of glass samples

Sample Code	*x*	ρ(g/cm^3)
S1	0	2.798
S2	4	2.912
S3	8	3.026
S4	11	3.111
S5	15	3.225

Table 2.2. Chemical composition(wt.%) of the glass samples

Constituent	S	S1	S2	S3	S4
	wt.%	wt.%	wt.%	wt.%	wt.%
CaO	0.2	0.2	0.2	0.2	0.2
$CoCl_2$	0.2	0.2	0.2	0.2	0.2
B_2O_3	0.25	0.25	0.25	0.25	0.25
P_2O_5	0.35	0.31	0.27	0.24	0.2
Fe_2O_3	0	0.04	0.08	0.11	0.15

2.2. Theoretical calculations

The attenuation of x-rays and gamma rays in a material can commonly be expressed using the exponential attenuation law. The basic equation is given by:

$$I = I_o e^{-\mu x} \tag{2.1}$$

Where:

I_o is the intensity (or number of photons) after passing through a distance x in the material,

I_o is the initial intensity (or number of photons) of the beam before entering the material,

μ is the linear attenuation coefficient of the material, which is a measure of how strongly the material can attenuate the beam through various interactions (including Compton scattering, photoelectric absorption, and pair production),

x is the thickness of the material that the photons are traveling through.

The linear attenuation coefficient (μ) can be considered as a combination of several contributions from different types of interactions. Each type of interaction contributes to the overall attenuation depending on the energy of the photons and the properties of the material. Further elaboration on the specific contributions to μ can be provided by separating it into relevant components:

$$\mu = \mu_{\text{coh}} + \mu_{\text{com}} + \mu_{\text{photo}} + \mu_{\text{pair}} \tag{2.2}$$

Where:

- μ_{coh} is the contribution from coherent (Rayleigh) scattering,

- μ_{com} is the contribution from Compton scattering,

- $\mu_{\text{photo}}$is the contribution from the photoelectric effect,

- $\mu_{\text{pair}}$is the contribution from pair production.

In this work, the partial interaction probability is calculated by dividing each partial contribution by μ.

In a narrow beam of monoenergetic photons, each Compton scattering results in the probability of a photon being taken out of the beam, similar to how absorption events remove photons from the beam. Each of these interactions will contribute to the overall attenuation and the way the intensity of the beam decreases as it interacts with the matter it passes through. This exponential nature of attenuation is foundational in fields such as medical imaging, radiation protection, and materials science.

The mass attenuation coefficient(μ_m in cm^2/g) provides a measure of how much a material can attenuate (reduce the intensity of) radiation per unit mass. It is a useful quantity in areas like medical imaging and radiation shielding, as it allows for comparisons of how different materials interact with various types of radiation based on their mass rather than their volume.

The mass attenuation coefficient is simply the linear attenuation coefficient divided by the density ρ (in g/cm^3) of the absorber:

$$\mu_m = \mu/\rho \tag{2.3}$$

where:

ρ is the density of the absorber (in $\mathrm{g/cm^{-3}}$).

The mass attenuation coefficients of compounds and mixtures, such as glass, concrete, and composites, can be calculated using software tools like NXcom (El-Khayatt, 2011), and WinXCom (Gerward et al., 2004). NXcom, reported by El-Khayatt, calculates fast neutron attenuation coefficients and the total and partial cross-sections for various photon interactions, including absorption and scattering. On the other hand, WinXCom developed by Gerward et al., determines the gamma ray mass attenuation coefficient ($\mu_m, \mathrm{cm}^2/\mathrm{g}$). Both programs utilize the "mixture rule," which states that the total attenuation results from the simple sum of contributions from individual components, as described in the following equations (El-Khayatt, 2011; Gerward et al., 2004):

$$(\mu_m)_{sample} = \sum_i w_i \, (\mu_m)_i \tag{2.4}$$

Here ρ_i denotes the density of the i^{th} constituent element in the sample, while w_i represents the weight fraction. The weight fraction of an element in a compound is found from

$$w_i = k_i A_i \, / A \tag{2.5}$$

where k_i is the number of ith atoms of the ith element, and A is the molecular weight of the compound.

2.3. Half Value Layer (HVL)

The half value layer (HVL) is the material thickness that reduces radiation intensity to half its original value. Higher linear attenuation values typically correspond to lower HVL values. HVL is calculated using the following equation (El-Khayatt and Akkurt, 2013):

$$x_{1/2} = \ln 2 \, / \mu \tag{2.6}$$

Chapter 3: Results and discussion

3.1. Linear attenuation coefficients

The elemental composition of various glass samples was input into the XCom program, to calculate the linear attenuation coefficient at different energies. Results are shown in Figures 3.1-3.3. Figure 3.1 illustrates how the linear attenuation coefficient (μ) varies with photon energy for the control glass sample (without Fe_2O_3).

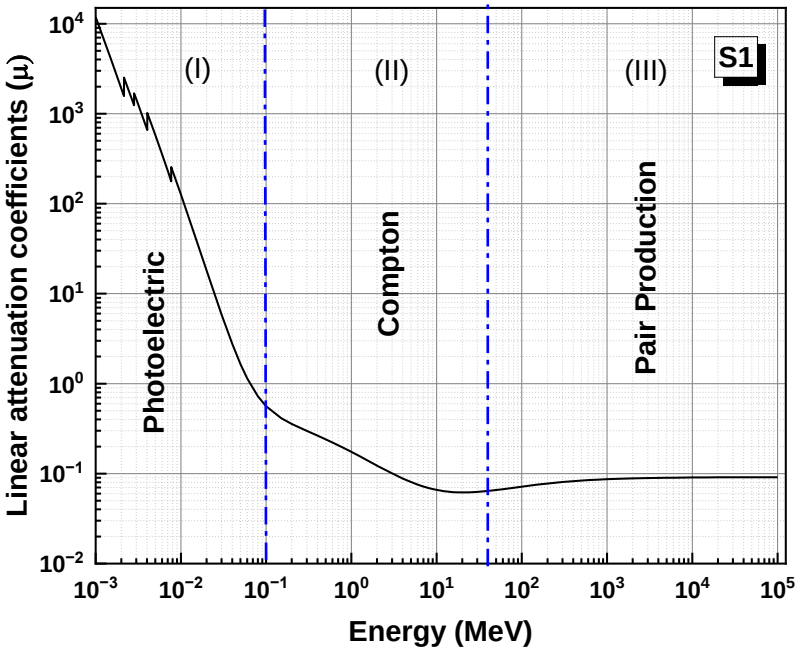

Figure 3. 1: Linear attenuation coefficients of photons in the S1 glass sample.

The variation of the linear attenuation coefficient in sample S1 will serve as an example for the other samples, classified into three regions. **In region I,** coefficients sharply decline with increasing photon energy for all glasses, mainly due to the photoelectric effect, which dominates between 0.01 and 0.1 MeV, while Compton scattering prevails from 0.1 to 100 MeV.

In region II, coefficients decrease slightly with rising photon energy across all samples, as Compton scattering predominates with a notable contribution from pair production. Compton scattering is the main interaction for low and intermediate atomic number elements from 1 to 10 MeV, with pair production becoming significant for atomic number 60 at 0.5 to 5 MeV.

In region III, coefficients slightly increase with higher photon energies due to repeated Compton scattering collisions, which reduce photon energy to levels that allow absorption via the photoelectric effect, resulting in a modest increase in the total cross-section.

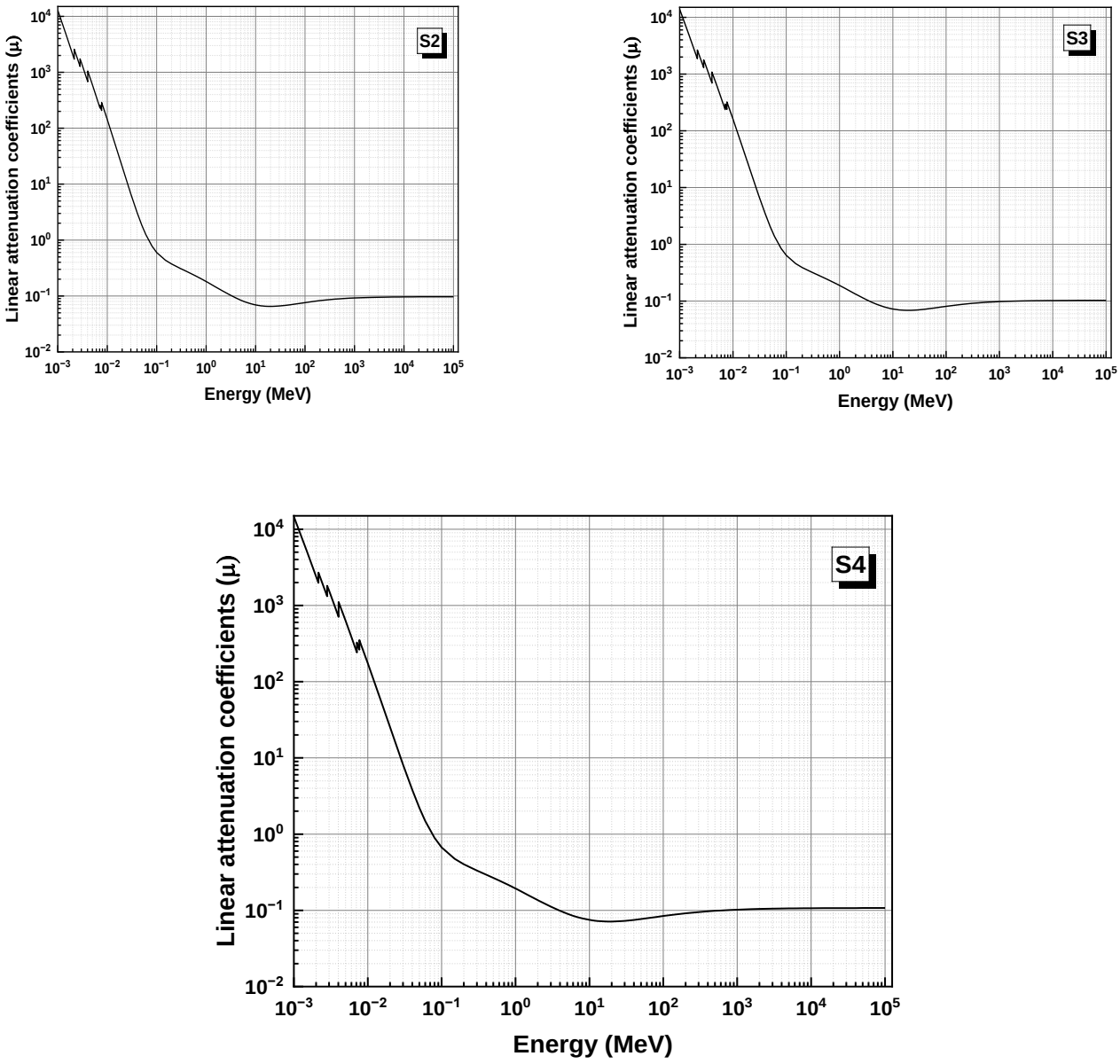

Figure 3.2: Linear attenuation coefficients the glass samples S2- S4.

Figure 3.3 illustrates the attenuation values of the control sample and the iron oxide-loaded sample simultaneously. The sample S5 consistently exhibits higher values

than the control sample S. Overall, linear attenuation coefficients decrease with increasing energy while rising with higher Fe_2O_3 content.

A notable feature in these figures is the discontinuity in the curves at low energy levels, caused by the K-absorption edges of elements with atomic numbers greater than 10, such as Ca, Co, and Fe, which complicate the μ-energy curves.

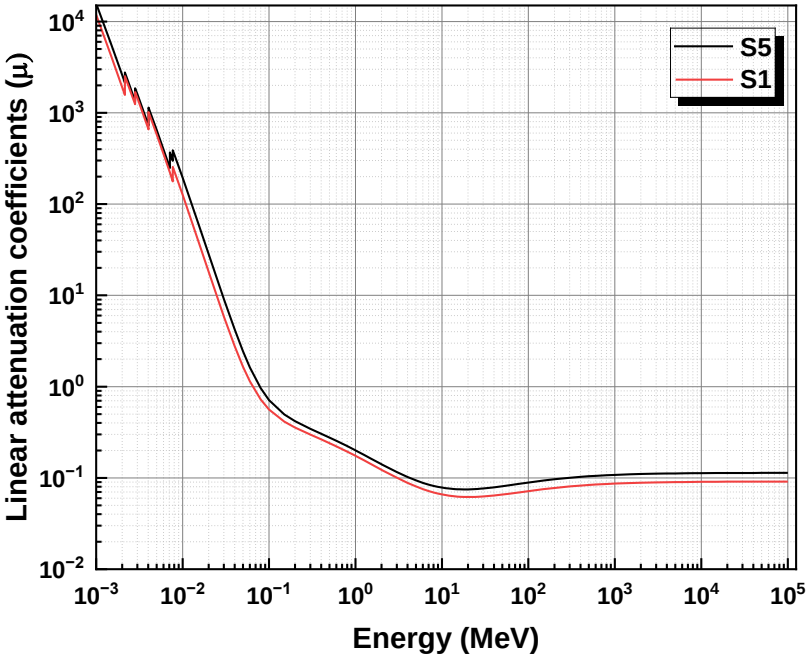

Figure 3.3: Linear attenuation coefficients of the glass samples S1and S5.

3.2. Half Value Layer (HVL)

To evaluate the shielding effectiveness of the glass samples, the half-value layers (HVL) were calculated and plotted in Figures 3-4. The S1 sample displayed higher HVL values, signifying lower attenuation ability compared to the S5 sample with greater Fe_2O_3 content. Additionally, lower HVL values were noted at intermediate and higher energy levels, where Compton scattering and pair production interactions dominate.

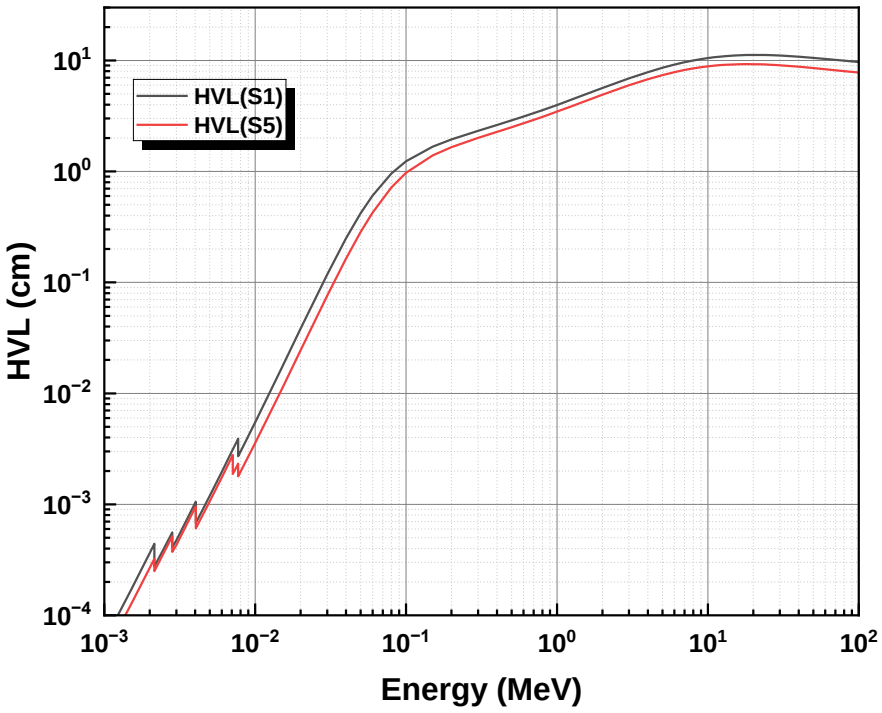

Figure 3.4: Half-Value Layer of the glass samples S1and S5.

3.3. Relative interaction probabilities

Figures 3.5-3.6 depict the interaction probabilities between 10 keV and 100 MeV. The curves indicate that Compton scattering predominates around 1 MeV, while photoelectric absorption and pair production are more significant at lower and higher energies, respectively. The intersection points indicate the energy values at which the probabilities of two interaction types are equal. Table 3.1 presents these energy values, where total interaction probabilities are evenly distributed between the two processes.

Table 1.3. Energies (in keV) at which the probabilities of two interaction types are equal.

Sample	Photoelectric & Compton	Compton & Pair production
S1	68	15.46
S2	70	15.18
S3	72	14.91
S4	74	14.67
S5	76	14.4o

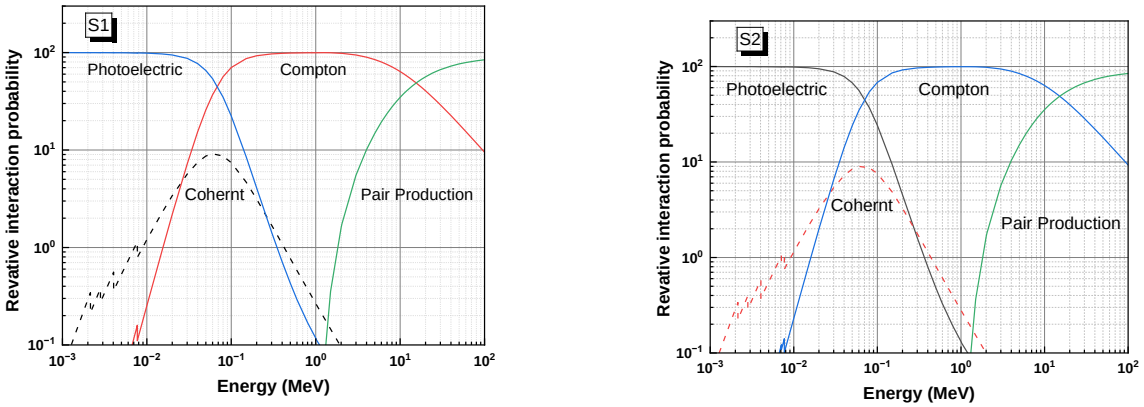

Figure 3.4: Relative interaction probabilities in the glass samples S1 and S2.

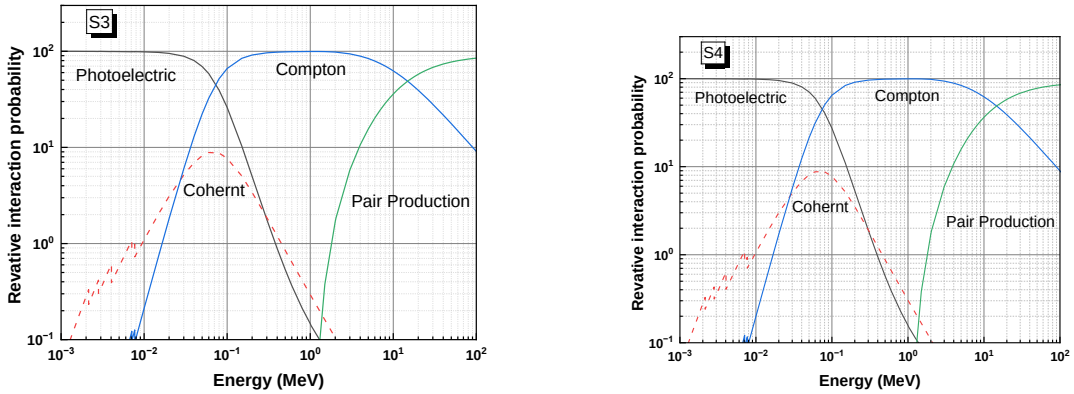

Figure 3.5: Relative interaction probabilities in the glass samples S3 and S4.

The results indicated that the equality points for photoelectric and Compton interactions shifted to higher energies, while the points between Compton and pair production moved to lower energies. This outcome is attributed to the increased effective atomic numbers of the glass samples due to the addition of Fe_2O_3.

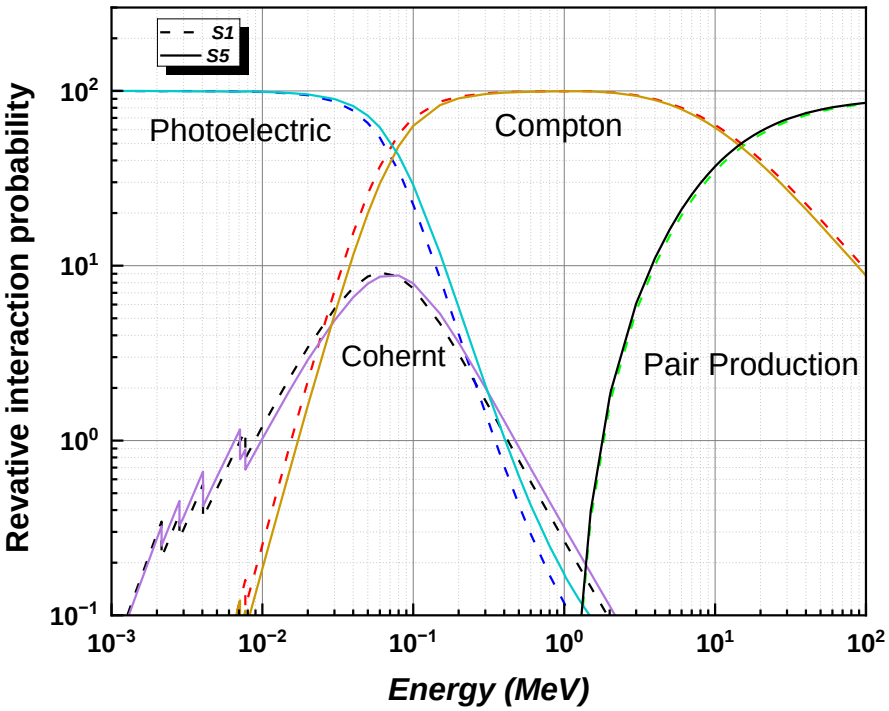

Figure 3.5: Relative interaction probabilities in the glass samples S3 and S4.

Conclusions

This study analyzes the relative attenuation probabilities of partial photon interactions in a five-glass system, identifying equal probability points (balance points) between the photoelectric effect and Compton scattering, as well as between Compton interactions and pair production. It calculates linear attenuation coefficients and half-value layers across a range of photon energies. Additionally, it examines the effect of replacing P_2O_5 with Fe_2O_3 in the glass system 20CaO-20$CoCl_2$-25B_2O_3 (35-x) P_2O_5-x Fe_2O_3 (where x=0, 4, 8, 11, and 15 wt. %). The findings demonstrate that this replacement enhances attenuation capacity, resulting in increased μ values, decreased HVL values, and a shift in the balance points of the partial interaction probabilities within the glass system.

References

El-Khayatt, A.M., 2017a. Water equivalence of some 3D dosimeters: A theoretical study based on the effective atomic number and effective fast neutron removal cross section. Nuclear Science and Techniques 28. https://doi.org/10.1007/s41365-017-0322-8

El-Khayatt, A.M., 2017b. Calculation of photon shielding properties for some neutron shielding materials. Nuclear Science and Techniques 28.

https://doi.org/10.1007/s41365-017-0222-y

El-Khayatt, A.M., 2017c. Semi-empirical determination of gamma-ray kerma coefficients for materials of shielding and dosimetry from mass attenuation coefficients. Progress in Nuclear Energy 98, 277–284. https://doi.org/10.1016/j.pnucene.2017.04.006

El-Khayatt, A.M., 2011. NXcom - A program for calculating attenuation coefficients of fast neutrons and gamma-rays. Ann Nucl Energy 38. https://doi.org/10.1016/j.anucene.2010.08.003

El-Khayatt, A.M., Akkurt, I., 2013. Photon interaction, energy absorption and neutron removal cross section of concrete including marble. Ann Nucl Energy 60. https://doi.org/10.1016/j.anucene.2013.04.021

El-Khayatt, A.M.M., Saudy, H.A.A., 2020. Preparation and characterization of zinc, lanthanum white sand glass for use in nuclear applications. Radiation Physics and Chemistry 166. https://doi.org/10.1016/j.radphyschem.2019.108497

El-Samrah, M.G., El-Mohandes, A.M., El-Khayatt, A.M., Chidiac, S.E., 2021. MRCsC: A user-friendly software for predicting shielding effectiveness against fast neutrons. Radiation Physics and Chemistry 182. https://doi.org/10.1016/j.radphyschem.2021.109356

Gerward, L., Guilbert, N., Bjørn Jensen, K., Levring, H., 2001. X-ray absorption in matter. Reengineering XCOM. Radiation Physics and Chemistry 60, 23–24. https://doi.org/10.1016/S0969-806X(00)00324-8.

Gerward, L., Guilbert, N., Jensen, K.B., Levring, H., 2004. WinXCom—a program for calculating X-ray attenuation coefficients. Radiation Physics and Chemistry 71, 653–654. https://doi.org/10.1016/j.radphyschem.2004.04.040.

Hubbell, J.H., Seltzer, S.M., 1995. Tables of X-Ray Mass Attenuation Coefficients and Mass Energy-Absorption Coefficients 1 keV to 20 MeV for Elements Z = 1 to 92 and 48 Additional Substances of Dosimetric Interest.